TABLE I. Summary of one-dimensional guard-ring disk data.

Shot[a]	u_p[b]	σ[c]	k[d]	i_t/i_i[e]	Tilt[f] factor	Configuration[g]
H-82	0.01744	2.64	2.04	···	0.45	A
H-77	0.02952	4.47	2.06	1.03	0.34	A
H-75	0.04547	6.89	2.09	1.01	0.27	A
H-74	0.05105	7.74	2.11	1.03	0.10	A
H-84	0.06072	9.20	2.12	1.05	0.11	A
H-78	0.06087	9.23	2.13	1.05	0.17	A
H-76	0.06975	10.57	2.13	1.04	0.09	A
H-71	0.07827	11.86	2.13	1.05	0.11	A
H-70	0.09214	13.97	2.15	[h]	0.09	A
H-72	0.09275	14.06	2.14	[h]	0.02	A
H-67	0.1028	15.58	2.16	1.05	0.09	A
H-88	0.1119	16.96	2.18	1.08	0.09	A
H-62	0.1137	17.23	2.18	1.06	0.13	A
H-89	0.1167	17.69	2.18	1.08	0.06	A
H-90	0.1252	18.98	2.23	1.08	0.08	A
H-61	0.1292	19.58	2.27	1.08	0.14	A
H-64	0.1337	20.26	2.27	1.08	0.09	A
P-231	0.0281	4.26	2.04[k]	[j]	0.64	C
P-241	0.0398	6.03	2.02	[j]	0.44	C
P-242	0.0465	7.05	2.10	1.03	0.25	C
P-243	0.0552	8.37	2.11[l]	1.05	0.33	D
P-227	0.0638	9.67	2.14[l]	1.03	0.20	C
P-251	0.0700	10.61	2.13	1.03	0.11	D
P-225	0.0941	14.26	2.17	1.05	0.20	C
P-228	0.1080	16.37	2.15	1.06	0.21	C
P-226	0.1197	18.14	2.16	1.05	0.36	C
P-234	0.1252	18.98	2.21	1.05	0.45	E
P-235	0.1270	19.25	2.25	1.05	0.43	F
P-237	0.1345	20.39	2.23	1.07	0.35	G
P-258	0.1440	21.83	2.24	1.10	0.16	C
P-229	0.1547	23.45	2.38	1.08	0.15	C
P-224	0.1555	23.57	2.26	1.07	0.12	H
P-259	0.1661	25.18[m]	2.29	1.08	0.10	C
P-230	0.2201	33.67[m]	2.41	[n]	0.23	C
P-261	0.2644	41.04[m]	2.48	1.21[n]	0.12	C
P-260	0.2672	41.51[m]	2.38	[o]	0.10	C
P-233	0.2886	45.01[m]	2.38	[o]	0.15	C
P-256	0.3118	48.82[m]	2.43	[n]	0.07	D

[a] H prefix indicates experiments on compressed-gas gun. P prefix indicates experiments on propellant gun. H experiments recorded on direct deflection 517 oscilloscopes with risetime 3 nsec. P experiments recorded on 545 oscilloscopes, L preamplifier, risetime 12 nsec.

[b] u_p is particle velocity at impact surface. Computed as one-half the measured impact velocity. Units are mm-μsec^{-1}.

[c] σ is impact stress ($\rho U_s u_p$), computed from particle velocity using $\rho=2.650$ g-cm^{-3} and $U_s=5.72$ mm-μsec^{-1}, except as noted. Units are kbars.

[d] k is the current coefficient computed from the expression $k=(l/Ac_{11})(i_i/u_p)$. The area is computed from the measured diameter of the inner electrode. Values of A and l are thus known to an accuracy of $\pm 0.1\%$. Bechmann's value $c_{11}=86.74\times10^{10}$ dyn-cm^{-2} is used for k computation from zero to 25 kbar and verified experimentally by the U_s readings. For stress greater than 25 kbar, c_{11} is computed from the expression $c_{11}=\rho U_s^2$, where $\rho=2.65$ g-cm^{-3} and U_s is the least-squares fit to the velocity measurements. Units are 10^{-8} C-cm^{-2}-kbar^{-1}.

[e] i_i is current jump. i_t is current at transit time. i_t/i_i is a measure of the increase in current during wave-transit time.

[f] The tilt factor is the ratio of the measured time to impact the electroded area to the wave-transit time.

[g]
A $1\frac{1}{2}$ in. o.d. 0.100 in. thick 0.6-in.-diam inner electrode
C $1\frac{1}{2}$ in. o.d. 0.100 in. thick 0.5
D $1\frac{1}{2}$ in. o.d. 0.125 in. thick 0.5
E $1\frac{1}{2}$ in. o.d. 0.100 in. thick 0.63
F $1\frac{1}{2}$ in. o.d. 0.100 in. thick 0.38
G $1\frac{1}{2}$ in. o.d. 0.100 in. thick 1.0
H $1\frac{1}{2}$ in. o.d. 0.150 in. thick 0.5

[h] Slight pressure increase prior to impact.

[j] Cannot measure current rise accurately due to large tilt values.

[k] k computed from integrated current.

[l] $-X$ orientation—no conductivity observed.

[m] Stress computed from $U_s=5.57+1.08u_p$ mm-μsec^{-1} which is the linear east-squares fit to the data above 25 kbar.

[n] Current–time observed is nonlinear.

[o] Current discontinuities before completed wave transit.

The observed current–stress relationship is expressed by defining a current coefficient

$$k=i_i l/\sigma A U_s=i_i l/u_p A c_{11}, \tag{8}$$

where i_i is the measured current jump and $c_{11}=\rho U_s^2$. The low-signal constant-field elastic-stiffness constant c_{11}^E given by Bechmann[14] was used in the computation of k for stress less than 25 kbar. For stress greater than 25 kbar an elastic stiffness coefficient was computed from the observed wave velocity given below. The experimental values of the current coefficient are k 2.04×10^{-8} C-cm^{-2}-kbar^{-1} for stress from zero to 6 kbar and $k=2.15\times10^{-8}$ C-cm^{-2}-kbar^{-1} from 9–18 kbar. All observed experimental points are within $\pm1.5\%$ of the mean values quoted. Above 18 kbar the coefficient is continuously variable. From these data we conclude that the limit of low-signal piezoelectric behavior for shock-loaded X-cut quartz is 6 kbar. This conclusion is further strengthened by the fully electroded data shown below.

In the low stress limit we obtain a direct measure of the piezoelectric stress constant e_{11}. From Eqs. (6)–(8), and an area correction for the effect of the ring, we find that

$$e_{11}=kc_{11}A/A_e, \tag{9}$$

where A is the area of the inner electrode and A_e is the effective area of the inner electrode. This is taken as A plus one-half the area of the insulating ring. Our value is compared to recent determinations by other authors[14,15] in Table II. It should be emphasized that

TABLE II. Observed piezoelectric stress constant e_{11}.

Present work	0.174 C-m^{-2}
Bechmann[14]	0.171
Koga *et al.*[15]	0.175

in the low stress limit, this technique gives e_{11} directly and that the value obtained is not dependent upon the value chosen for the elastic stiffness. It should also be emphasized that the current coefficient was computed from the area of the inner electrode; therefore, the inner electrode area, not A_e, should be employed in Eq. (6) when using the quartz disk as a gauge.

From the transit time indicated on the current–time record we obtain a direct measure of the propagation velocity in the single wave region. The least-squares fit to the U_s vs u_p data is

$$0<\sigma<25 \text{ kbar} \quad U_s=5.740 (s=0.04) - 0.14u_p (s=0.24) \text{ mm-}\mu\text{sec}^{-1}$$
(23 observations),

$$25<\sigma<50 \text{ kbar} \quad U_s=5.57 (s=0.10) + 1.08u_p (s=0.44) \text{ mm-}\mu\text{sec}^{-1}$$
(12 observations),

where s is the standard deviation.

[14] R. Bechmann, Phys. Rev. **110**, 1060 (1958).

[15] I. Koga, M. Aruga, and Y. Yoshinaka, Phys. Rev. **109**, 1467 (1958).

The fit from atmospheric pressure to 25 kbar shows that the wave velocity changes less than $\frac{1}{2}\%$ with a mean value of 5.728 mm/μsec. Hence, the current coefficient determination which relates current to stress is accomplished with an estimated accuracy of $\pm 3\%$ in the stress range to 25 kbar.

The standard deviations of the coefficients for the wave velocity least-squares fit for stress amplitude greater than 25 kbar are large; however, a comparison of computed values from our least-squares fit with those of Wackerle[8] (Table III) shows excellent agreement.

TABLE III. Comparison of least-squares fit to wave velocity determination above 25 kbar.

u_p	U_s Wackerle	U_s Present work
0.1661 mm-μsec^{-1}	5.76 mm-μsec^{-1}	5.75 mm-μsec^{-1}
0.2201	5.81	5.81
0.2644	5.85	5.86
0.2672	5.85	5.86
0.2886	5.87	5.88
0.3318	5.89	5.91

For the stress region above about 30 kbar the current from the disk is generally less predictable and shows nonlinear current–time effects apparently due to dielectric permittivity changes and conduction. These effects limit accurate use of the guard-ring disk as a gauge to the measurement of stress jumps.

In agreement with previous observations on bounded disks,[16] internal conduction is observed for quartz in the $-X$ orientation in the guard-ring gauge configuration. Conduction does not occur for the $+X$ orientation guard-ring disk for the stress range up to about 30 kbar. The $+X$ orientation is obtained by orienting the disk such that a compressive stress wave propagates from the $-X$ electrode to the $+X$ electrode. The polarity of the electroded faces of the disk is determined with the gauge in compression. For a quantitative analysis of the effect of finite resistivity on piezoelectric current the reader is referred to Wittekindt.

FULLY ELECTRODED DISKS

For many experiments a fully electroded disk can be used as a gauge if the resulting distortion of the current waveforms is known; for example, the results of Jones *et al.*[1] were obtained with the fully electroded gauge. The gauge is constructed from an X-cut quartz disk in a manner similar to the guard-ring gauge, except that the guard ring is not formed and the $+X$ electrode is placed in direct contact with an aluminum disk that has the same diameter as the quartz. Electrical connection is made to the aluminum disk.

Typical records obtained with a step input of stress into various fully electroded disks are shown in Fig. 6. The pronounced distortion in current compared to the current from the guard-ring configuration is apparent. The extent of the distortion depends upon the particular d/l ratio of the disk and, as expected, is more pronounced for the gauges with a smaller d/l ratio.

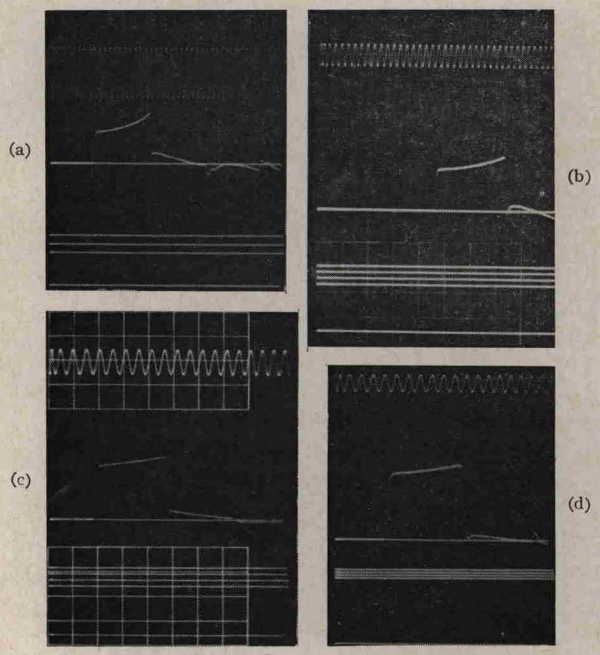

FIG. 6. Typical current–time records from various diameter-to-thickness ratio disks. Time increases from left to right. (a) $d/l=2$, Shot H-56B, 10-Mc/sec timing wave. (b) $d/l=4$, shot 97C, 5-Mc/sec timing wave. (c) $d/l=10$, shot 104B, 10-Mc/sec timing wave. (d) $d/l=16.7$, shot 79A, 5-Mc/sec timing wave.

If tilt is negligible the current jump at impact time should not be affected by unloading waves from the lateral boundary. However, distortion to this current jump can be caused by electrostatic field distortion. Early in the propagation time the stressed region is very thin with the result that the field lines in the stressed portion are not severely distorted. The unstressed region, however, is relatively thick and, depending upon the d/l ratio of the disk, considerable distortion to the field lines will be present. The effect of the field fringing on the current jump is analyzed in the Appendix by considering the relative field fringing between the stressed and unstressed regions of the disk. This relative field fringing has the same effect as a difference in permittivity between the two regions causing the current jump to be depressed below that predicted for the one-dimensional case. As the wavefront progresses through the disk the relative field distortion between the stressed and unstressed regions of the disk changes until, finally, at wave-transit time the unstressed region is relatively undistorted and the stressed region shows distortion. Late in the first-wave transit we would also expect the piezoelectric response due to the unloading waves from the lateral boundaries

[16] R. A. Graham, J. Appl. Phys. 33, 1755 (1962).
[17] R. H. Wittekindt, Harry Diamond Laboratory Report No. TR-922 (May 1961).